

Anomalous layering of Fe(CO)₅ adsorbed on graphite

J. R. Dennison, H. Taub, and F. Y. Hansen*

Department of Physics and Astronomy, University of Missouri-Columbia, Columbia, Missouri 65211

H. Shechter and R. Brener

*Department of Physics and Solid State Institute, Technion-Israel Institute of Technology,
32000 Haifa, Israel*

(Received 17 April 1987)

Synchrotron x-ray diffraction experiments reveal the adsorption of iron pentacarbonyl [Fe(CO)₅] on graphite basal-plane surfaces to be an extreme example of incomplete wetting in which only one solid layer of film coexists with bulk particles. Upon heating through the monolayer melting point, the amount of coexisting bulk solid first *increases* and then decreases. This anomalous layering behavior has not been observed in other systems exhibiting incomplete wetting, and we suggest that it is related to the steric properties of the Fe(CO)₅ molecule.

The manner in which physically adsorbed films grow on solid surfaces has been a subject of intense theoretical and experimental activity in the last few years. The vast majority of films are known to incompletely wet a substrate at low temperature.¹ That is, only a finite number of layers n adsorb before the nucleation of bulk particles. Some incompletely wet systems undergo a series of layering transitions in which n increases in discrete steps at successively higher temperatures.² If an infinite number of layers forms, the wetting is said to be complete.

Despite the prevalence of incomplete wetting, little is known about mechanisms other than layering transitions, which can affect the distribution of molecules between the coexisting bulk and film phases. For example, one can ask whether the bulk amount is conserved when the film changes state such as at melting. If the fluid film has a lower density than the solid, are the excess molecules accommodated within the film by promotion to higher layers or is there a transfer of molecules to the bulk phase? In the most extensively studied example of incomplete wetting, ethylene on graphite,³⁻⁵ the quantity of bulk did not change at the film melting point but only decreased at each layering transition.

Previous neutron-diffraction experiments with iron pentacarbonyl [Fe(CO)₅] adsorbed on graphite⁶ have suggested a qualitatively different layering behavior than that of ethylene. However, these measurements were hampered by low scattered intensities and poor wave-vector (Q) resolution. We have recently reexamined this system using synchrotron x-ray diffraction which has clarified the layering behavior and allowed it to be described quantitatively. Our principal findings are (1) only one solid layer of Fe(CO)₅ wets the graphite basal-plane surface; (2) the decrease in monolayer density upon melting results in an *increase* in the amount of coexisting bulk solid rather than promotion of molecules to a second film layer; and (3) at still higher temperatures, but below the bulk triple point, a *decrease* in the bulk amount occurs as the result of a layering transition to a bilayer fluid. Here we summarize the evidence for this anomalous layering behavior and suggest that its origin is in the unusual steric properties of the bipyramid-shaped Fe(CO)₅ molecule.

X-ray diffraction experiments were performed at the National Synchrotron Light Source (NSLS) at the MATRIX⁷ beam line X18a using a double (flat) Si(111) monochromator set at a wavelength of 1.4 Å. Soller collimation between the sample and detector yielded a Q resolution of $\sim 0.02 \text{ \AA}^{-1}$ full width at half maximum. Diffraction scans were performed in transmission through a flat-plate copper cell 1.2 cm thick fitted with Be windows. Two cells containing 1.2 g of cleaned exfoliated graphite (Papyex) were filled at room temperature to $f=1.6$ and 2.3 layers⁸ of Fe(CO)₅, respectively, and then sealed. The Papyex substrate had a specific surface area of 21 m²/g and an average basal-plane coherence length of $\sim 240 \text{ \AA}$.

Our previous neutron experiments⁹ showed that the submonolayer solid forms a commensurate (C) herringbone structure in which the molecules are oriented with one of their bipyramid faces parallel to the graphite basal-plane surface. We found that this phase underwent an orientational disordering (OD) transition prior to melting similar to that observed for the herringbone structures of nitrogen¹⁰ and ethane¹¹ on graphite. The commensurate, orientationally-disordered, and fluid submonolayer phases of Fe(CO)₅ are denoted C, OD, and F, respectively, in the phase diagram of Fig. 1.

X-ray diffraction patterns from 1.6 and 2.3 layers of Fe(CO)₅ on Papyex are plotted in Fig. 2 as a function of temperature. Scattering from the Papyex is featureless [except near the graphite (002) peak at $Q=1.9 \text{ \AA}^{-1}$ where data are omitted] and has not been subtracted from the patterns. Below 173 K, the patterns are dominated by a Bragg peak at $Q=1.20 \text{ \AA}^{-1}$ which profile analysis shows has the asymmetric Warren line shape¹² expected for a polycrystalline monolayer. The peak position is 7.5% higher in Q than the similarly intense {20} peak of the commensurate phase. From this peak shift, we infer that the monolayer has been compressed into an incommensurate phase denoted by I in Fig. 1 (Ref. 13). Assuming isotropic compression as in the densest monolayer phases of N₂ (Ref. 10) and ethane,¹¹ the I-phase areal density is about 15% greater than that of the C phase.¹⁴

We infer the melting of the incommensurate phase

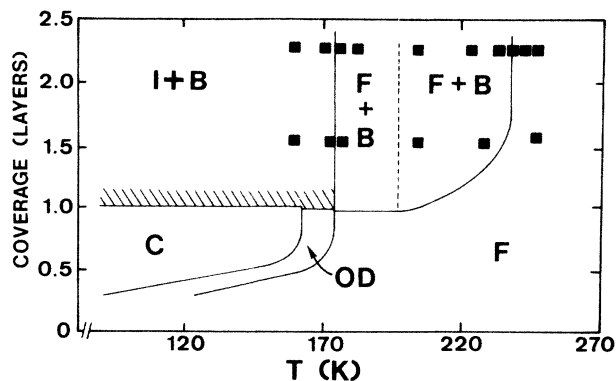


FIG. 1. Proposed phase diagram for $\text{Fe}(\text{CO})_5$ on graphite. Squares correspond to x-ray diffraction scans. See text for definition of the phases. Dashed line indicates onset of fluid monolayer-to-bilayer transition.

from the dramatic change in the diffraction pattern at 175 K in Fig. 2(a). The most prominent I-phase peak at $Q = 1.20 \text{ \AA}^{-1}$ and a weaker peak at $Q = 1.03 \text{ \AA}^{-1}$ have disappeared. In addition, there is now a broad component in the scattering, most easily seen at low Q , which can be attributed to a fluid monolayer. The peaks in the low-temperature patterns of Fig. 2(a) which remain above the I-phase melting point, can be identified with coexisting bulk $\text{Fe}(\text{CO})_5$ denoted B in Fig. 1. In Fig. 2(c), we see that these peaks sharpen and intensify in the 2.3-layer

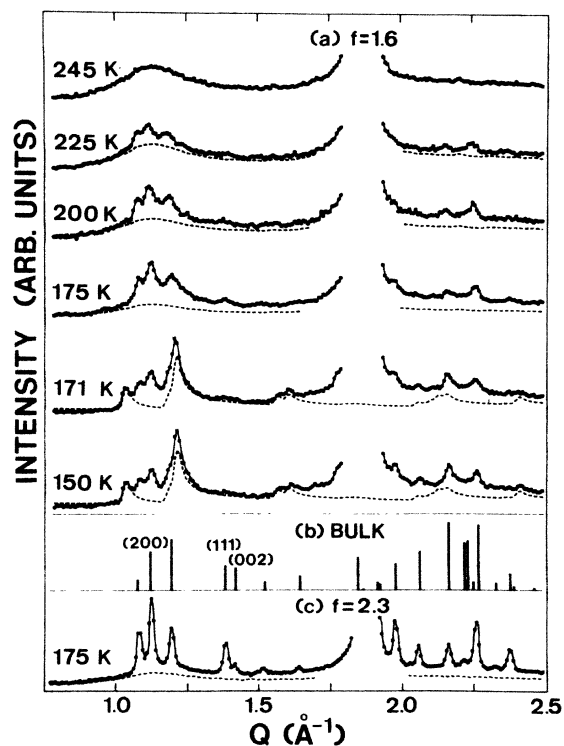


FIG. 2. X-ray diffraction scans as a function of temperature: (a) 1.6-layer sample and (c) 2.3-layer sample. Calculated pattern for an isotropic powder of bulk $\text{Fe}(\text{CO})_5$ is in (b).

sample at 175 K. Their positions are in excellent agreement with those predicted for an isotropic powder of bulk monoclinic¹⁵ $\text{Fe}(\text{CO})_5$ as shown in Fig. 2(b).¹⁶ Between 190 K and ~ 230 K, these bulk peaks weaken and the intensity of the monolayer fluid component increases. By 245 K, the bulk peaks have completely disappeared in both the 1.6- and 2.3-layer samples. Since 245 K is below the bulk triple point at 252 K, we conclude that a layering transition from one to two layers of fluid has occurred as discussed below.

In order to proceed with a more detailed analysis of the layering behavior, it is necessary to separate quantitatively the solid monolayer, fluid film, and bulk contributions to the diffraction patterns in Fig. 2. For temperatures from 175 to 225 K in Fig. 2(a), the dashed curves represent our estimate of the fluid film component in the pattern. They were obtained by scaling the pure fluid profile at 245 K to fit the long leading edge of the lower-temperature patterns.¹⁷ The difference between the observed pattern and the dashed curve is then the scattering contribution from the bulk particles. At temperatures ≤ 171 K, the dashed curves represent the contribution to pattern from the solid monolayer incommensurate phase. They are calculated by subtracting the bulk contribution from the observed pattern. This was obtained by scaling the bulk pattern inferred at 175 K (see above) until it fit the most intense bulk peaks at each temperature.

We now focus on the behavior of the two samples near the melting point of the incommensurate phase, $T_m = 173$ K. The integrated intensity of the strongest incommensurate phase peak at $Q = 1.20 \text{ \AA}^{-1}$ plotted versus temperature is shown in Fig. 3(a). Data from both the 1.6-layer sample in Fig. 2(a) (circles) and the 2.3-layer sample (squares) have been included. In addition, there are data from the 1.6-layer sample (triangles) taken at more closely spaced temperature intervals but in a narrower Q range about the peak of interest. For all three data sets, the bulk and fluid contributions to the scattering have been subtracted as described above. The peak intensity changes abruptly near T_m and shows hysteresis as the temperature is varied in opposite directions. We find a width to the transition of ~ 6 K, implying that the melting is first order. A complementary plot in Fig. 3(b) monitors the amount of fluid film. The integrated intensity $I(\Delta Q)$ from a small Q range ΔQ near $Q = 1 \text{ \AA}^{-1}$, just below the lowest Bragg peaks of the bulk and monolayer incommensurate phases, is plotted as a function of temperature. As expected, there is an abrupt rise in $I(\Delta Q)$ upon heating which coincides with the drop in the monolayer peak intensity in Fig. 3(a). Moreover, in agreement with the interpretation of a layering transition, there is another rise in $I(\Delta Q)$ near 240 K where the bulk peaks completely disappear. This rise is more pronounced in the 2.3-layer sample.

Next, we examine the quantity of coexisting bulk material near T_m . Following previous studies,⁴ we assume that it is proportional to the integrated intensity of a bulk Bragg peak. In Fig. 3(c), we have plotted the integrated intensity of the (200) peak versus temperature for the 1.6-layer sample (circles) as determined from the diffraction patterns in Fig. 2(a).¹⁷ This peak was selected

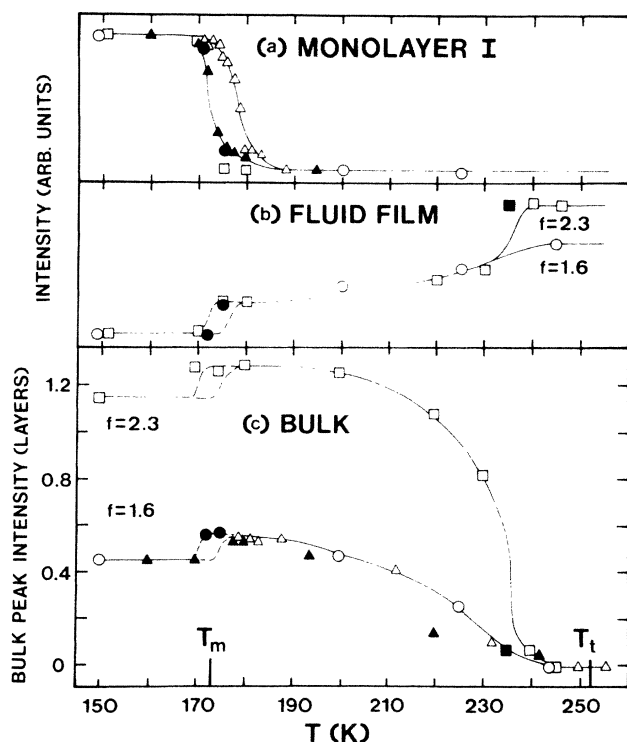


FIG. 3. (a) Integrated intensity of the strongest Bragg peak ($Q = 1.20 \text{ \AA}^{-1}$) in the monolayer I phase vs temperature. Data from the 1.6- and 2.3-layer samples have been scaled to the same value at 150 K. (b) Temperature dependence of the fluid film intensity $I(\Delta Q)$ defined in the text. Data of the two samples have been scaled so that at 245 K the ratio of $I(\Delta Q)$ is that of the total coverage. (c) Temperature dependence of the bulk peak intensity as described in the text. Throughout the figure, data for the 1.6-layer sample are shown by circles and triangles while squares are used for the 2.3-layer sample. Open and closed symbols indicate increasing and decreasing temperature, respectively. The solid lines are guides to the eye. The dashed lines in (b) and (c) indicate the hysteresis region determined from (a).

because it is the most intense bulk peak, and it is well separated from those of the monolayer incommensurate phase. At 150 K, the (200) intensity has been scaled to a value of $f = 0.45$ layers, an amount equal to the total coverage $f = 1.6$ less the material in the incommensurate phase.

Remarkably, we find that the bulk peak intensity *increases* by an amount corresponding to 0.11 layers⁸ just above T_m . This increase is confirmed by data (triangles) in Fig. 3(c) taken from scans at more closely spaced temperature intervals but in a smaller Q range about the (200) peak. For these data, points within the hysteresis loop of Fig. 3(a) have been excluded due to difficulties in subtracting the fluid film contribution. Also, data in Fig. 3(c) (squares) from scans on the 2.3-layer sample show the same 0.11-layer bulk increase between 150 K and T_m . Although there is only one point below T_m , the uncertainty in this data is less than for the 1.6-layer sample, since

each point is proportional to the total integrated intensity of three bulk peaks, the (200), (111), and (002).

The bulk increase at the monolayer melting point implies that the bulk free energy is lower than that of the fluid bilayer. We suggest that this results from the steric properties of the $\text{Fe}(\text{CO})_5$ molecule. In order to overcome steric hindrance to rotation about a surface normal, an appreciable density change probably occurs upon melting of the compressed incommensurate phase. An accurate estimate of the monolayer fluid density is difficult to obtain from the single broad peak in its diffraction pattern, but a reasonable upper bound would be that of the commensurate OD phase⁹ which is 15% less dense than the incommensurate phase. Monolayer melting thus produces an excess of fluid molecules which, instead of being promoted to a second layer, apparently migrate to bulk. Due to the large barrier to rotation about an axis parallel to the surface, the molecules in the fluid monolayer probably maintain a bipyramid face next to the surface (as in the solid commensurate and OD phases) while undergoing random translational motion. This residual orientational order in the monolayer fluid could inhibit growth of a second layer just as in the case of the solid incommensurate phase. Migration of 15% of the molecules in the incommensurate phase to bulk would be equivalent to a 0.17-layer bulk increase. Since some of these molecules may form very small particles whose Bragg peaks would be too broad to be observed, the 0.11-layer effect which we have inferred from Fig. 3(c) is still consistent with this interpretation. The gradual increase in the amount of fluid film above 190 K at the expense of the coexisting bulk solid may also be understood qualitatively in terms of steric effects. At these higher temperatures, the molecules in the fluid monolayer could begin to rotate about an axis parallel to the surface, thereby providing a smoother template on which to grow a second layer.

To our knowledge, a bulk increase upon melting of the film has not been found previously in other cases of incomplete wetting. Likely candidates would be systems such as benzene on graphite¹⁸ in which only a single solid layer wets the surface and in which the monolayer melting point is well below that of bulk. While steric effects are expected to be more pronounced for the bipyramid-shaped $\text{Fe}(\text{CO})_5$ molecule, our results suggest they may be important in understanding the layering behavior of other nonspherical molecules.

The authors are indebted to J. G. Dash, L. Passell, E. Conrad, and particularly M. Wortis for discussing the interpretation of these experiments. We thank D. Chapman for his assistance at the National Synchrotron Light Source. This work was partially supported by the U.S. National Science Foundation Grants No. DMR-79-05958, No. DMR-83-04366, and No. DMR-87-04938; Israel-U.S. Binational Science Foundation Grant No. 2687; and U.S. Department of Energy Grant No. DE-FG02-85ER45183 of the MATRIX Participating Research Team.

*Present address: Fysisk-Kemisk Institut, The Technical University of Denmark, DK-2800 Lyngby, Denmark.

¹See, e.g., M. Bienfait, *Surf. Sci.* **162**, 411 (1985), and references cited therein.

²R. Pandit, M. Schick, and M. Wortis, *Phys. Rev. B* **26**, 5112 (1982).

³J. Menaucourt, A. Thomy, and X. Duval, *J. Phys. (Paris) Colloq.* **38**, C4-195 (1977).

⁴M. Sutton, S.G.J. Mochrie, R.J. Birgeneau, D.E. Moncton, and P.M. Horn, *Phys. Rev. B* **30**, 263 (1984).

⁵S.K. Satija, L. Passell, J. Eckert, W. Ellenson, and H. Patterson, *Phys. Rev. Lett.* **51**, 411 (1983).

⁶D.G. Reichel, D. Bahm, H. Taub, H. Shechter, and R. Brener, *Bull. Am. Phys. Soc.* **29**, 267 (1984).

⁷Midwest Analytical Team for Research Instrumentation of X Rays.

⁸Unity coverage $f=1$ is defined to be a complete layer of the commensurate $(\sqrt{7}\times\sqrt{21})19^\circ$ phase. Note that this definition differs from that in Ref. 9 which assumed a monolayer areal density about 20% lower.

⁹R. Wang, H. Taub, H. Shechter, R. Brener, J. Suzanne, and F.Y. Hansen, *Phys. Rev. B* **27**, 5864 (1983).

¹⁰R.D. Diehl and S.C. Fain, Jr., *Surf. Sci.* **125**, 116 (1983).

¹¹J. Suzanne, J.L. Seguin, H. Taub, and J.P. Biberian, *Surf. Sci.*

125, 153 (1983).

¹²B.E. Warren, *Phys. Rev.* **59**, 693 (1941).

¹³The detailed nature of the C-I transition is unknown (see shaded region in Fig. 1). We have not determined the order of the transition nor whether it proceeds initially via a uniaxial compression as in the case of N₂ on graphite (Ref. 10).

¹⁴This value of the density is corroborated by a Rietveld-type profile analysis of the I-phase diffraction pattern. The best fit to the dashed curve at 150 K in Fig. 2(a) is obtained for an incommensurate herringbone structure with a unit cell which is isotropically compressed from that of the C phase and slightly oblique.

¹⁵A.W. Hanson, *Acta Crystallogr.* **15**, 930 (1962).

¹⁶As in the case of ethylene adsorbed on graphite, the observed bulk peak intensities agree poorly with those calculated for an isotropic powder. As suggested in Ref. 5, this may be due to preferential orientation of the bulk crystallites on the graphite basal-plane surfaces.

¹⁷Our method of fluid subtraction neglects thermal expansion of the fluid film. If present, the broad fluid peak would shift to lower Q tending to increase our estimate of the bulk peak intensity.

¹⁸P. Meehan, T. Rayment, R.K. Thomas, G. Bomchil, and J.W. White, *J. Chem. Soc. Faraday Trans. I* **76**, 2011 (1980).